

# Study on the influence of blade outlet angle on unsteady flow and structural dynamic characteristics for chemical process pump

J F Zhang<sup>1</sup>, X Zhang<sup>1</sup> and L H Xie<sup>1</sup>

<sup>1</sup>National Research Centre of Pumps, 301 Xuefu Road, Zhenjiang, Jiangsu, 212013, China

759394263@qq.com

**Abstract.** In order to reveal the influence of the blade outlet angle on the structural dynamic characteristics of chemical process pump, a chemical process centrifugal pump with high specific speed was selected to be researched, and 4 impellers with different blade outlet angle were redesigned based on the prototype pump, which ensuring that the other geometrical parameters unchanged. The blade outlet angle designed are 27 °, 37 °, and 47 °, referring to the original impeller whose blade outlet angle was 22 °. Then, the numerical calculation was applied for each scheme under designed condition based on the bidirectional coupling fluid-structure interaction (FSI) simulations. Through simulation, the head after the fluid-solid coupling was lower than before, but the error was reduced. Comparing the distribution of equivalent stress at intersection boundary, it shows that the places from 0.6 times to 0.8 times at the outlet of the intersection boundary of stress side and shroud were greatly affected by blade outlet angle, and the places from 0.8 times at the outlet to the outlet at the intersection boundary of stress side and shroud were also greatly affected by blade outlet angle. In addition, the equivalent stress increases with the increasing of blade outlet angle, and the place near the outlet all tend to have the phenomenon of stress concentration. Moreover, the total deformation shows, the deformation could be reduced through reducing the blade outlet angle. Also, the structural behaviour of the impeller indicates the first-order inherent frequency was much higher than the blade frequency, and it avoided the second harmonic frequency and the third harmonic frequency. The inherent frequency could be improved when the blade outlet angle was relatively bigger, but if it was too big, it would cause swing and twist, and if it was lesser, the total deformation could be uniform.

## 1. Introduction

Chemical process centrifugal pump is the generic terms of all kinds of pump in the process of chemical production, and it is one of the largest rotating equipment in the chemical production equipment usage. Its work environment is relatively poor, so the performance requirements of the chemical pump are also very strict, once the chemical pump cannot work, it is likely to cause the paralysis of chemical process, and bring heavy losses<sup>[1]</sup>. The impeller is as the key flow passage components in the pump, and its reliability is very important to the process stability. Many scholars had done research on the optimization of the impeller parameters. Huang<sup>[2]</sup> et al researched the effect of the blade wrap angle on the external characteristics and the internal characteristics of the centrifugal pump. Zhang<sup>[3]</sup> et al did the whole flow field analysis on the various schemes with different blade number and different splitter length, and summarized their influence on the hydraulic performance of



the pump. These methods give detailed illustration on the impeller parameters, like inlet diameter, wheel hub diameter, inlet/outlet setting angle, blade number, and blade outlet width<sup>[4,5]</sup> et al.

From the existing literature, although there are a large number of studies focused on the effect of the blade outlet angle on the performance of the pump, the main teaching materials<sup>[6]</sup>, manuals<sup>[7]</sup> and reference books<sup>[8]</sup> in pump industry still continue to use the traditional theory to explain that the blade outlet angle has great influence on the performance of a centrifugal pump<sup>[9-11]</sup>, and the innovative research results are quite less.

This study focused on the influence of the blade out angle on the performance of the chemical centrifugal pump. The influence of the blade outlet angle on the external characteristic, internal characteristics, and pressure fluctuation were analyzed through the numerical simulation and experiments. In addition, the bi-directional coupling fluid-structure interaction (FSI) simulation was applied for revealing the effect of the blade outlet angle on the structure dynamic characteristics of the centrifugal pump.

## 2. Numerical Simulation and experiment validation

### 2.1. Computational model

The research object of this study is a high specific centrifugal pump for chemical process, and the main parameters are as following: the designed flow capacity  $Q=620\text{m}^3/\text{h}$ , delivery lift  $H=28\text{m}$ , impeller speed  $n=1450\text{r}/\text{min}$ .

**Table 1.** Main parameters of the chemical centrifugal pump model (unit, mm)

Parameter	Symbol	Value	Parameter	Symbol	Value
Blade number	Z	5	Blade outlet width	$b_2$	54
Impeller inlet diameter	$D_j$	225	Volute base circle diameter	$D_3$	355
Impeller outlet diameter	$D_2$	340	Blade outlet angle	$\beta_2$	$22^\circ$

In this paper, on the premise of guaranteeing other blade geometry parameters unchanged, three other impellers with different blade outlet angle:  $27^\circ$ ,  $37^\circ$ ,  $47^\circ$  were designed. The model contains three domains: the stationary inlet, the impeller, and a stationary volute. The gap part between the impeller and the volute was added in the volute water part in order to facilitate the division of the mesh. For making the flow develop well, the inlet and outlet pipes of the model pump were appropriately extended to increase the accuracy of the calculation<sup>[12]</sup>. In the end, the 3D shape of the components and the local detail chart of the volute casing were obtained.

### 2.2. Computational result

The outer characteristic test was carried out on the model pump with the blade outlet angle of  $22^\circ$  to verify the accuracy of the simulation. For conveniently using in the engineering, the dimensionless method was used to define the discharge coefficient  $\varphi$ , which was the reciprocal of the Strouhal number— $S_r$ :

$$\varphi = \frac{1}{S_r} = \frac{Q_v}{D_2^3 n} \quad (1)$$

The head coefficient number  $\psi$  was defined as:

$$\psi = \frac{gH}{u_2^2} \quad (2)$$

where, the  $D_2$  presents the impeller diameter,  $n$  is the impeller speed, and  $u_2$  is circumferential velocity.

Figure 1 shows the comparison of the simulation and experiment for the head. The discharge coefficient and head coefficient under the designed condition are 0.181, 0.397 respectively. From the figure, it is can be seen that the simulation head is all higher than the test head under the six conditions, and this may because the effect that the solid domain on the fluid domain is not considered. We can see the fitting degree is the best under the designed condition, and the error is lower than 2%.The error is biggest under the over load condition, and it is about 7%.This phenomenon shows the complex flow phenomenon like secondary flow, reflux easily will occur under the over load condition. As a whole, the difference between test and simulation is reasonable.

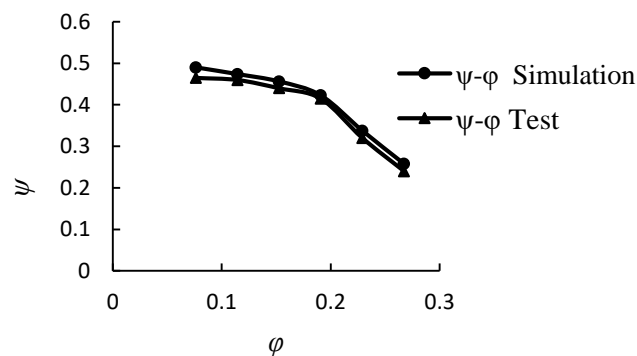


**Figure 1.** External performance experiment and numerical simulation of centrifugal pump

### 3. Characteristic analysis

#### 3.1. External characteristics analysis

Figure 2 shows the hydraulic performance for the four pumps with different blade outlet angle by numerical simulation. The figure indicates that appropriate increase of the blade outlet angle can improve head, when the angle increases to 47 °, the head under all the conditions decreases, and this may due to the severe curvature of the flow passage. Furthermore, the flow passage becomes significantly shorter, and the hydraulic loss increases, and the efficiency drops sharply, especially under the over load condition, and this may because of the serious blockage in the flow passage. Through the external analysis, it is necessary to increase the blade outlet angle based on the model pump to improve the hydraulic performance. In addition to this, it is also vertical to do further research on the reasonable value of the blade outlet angle based on the external characteristics.

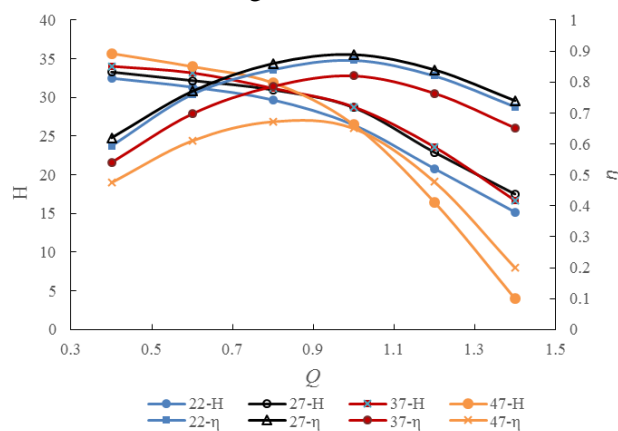


**Figure 2.** Performance curves of pump with different blade outlet angle

#### 3.2. Internal flow field analysis

The model pump was used for the chemical process, and it need to operate under the off design condition. Therefore, the off design performance of the four impellers was analyzed to investigate the influence of the blade outlet angle on the internal flow field of model pump.

*3.2.1. The distribution of regularization helicity.* In order to reveal the influence of the blade outlet angle on the internal flow of the impeller, the regularization helicity was introduced to extract the core line of vortex, and it was defined as:

$$H_n = \frac{\mathbf{i} \cdot \mathbf{u} \times \nabla \omega}{|\mathbf{v}| |\boldsymbol{\omega}|} \quad (3)$$

The distribution of the regularization helicity on the middle section of the impellers with different blade outlet angle under the different conditions are shown in the figure 3.

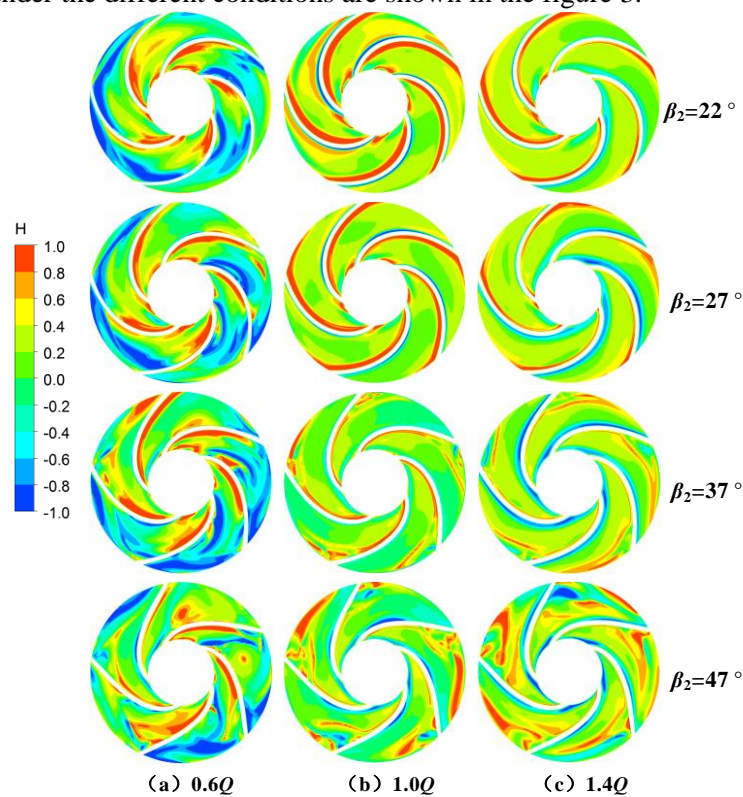


**Figure 3.** Distribution of  $H_n$  on the medium section of impellers with different blade outlet angles under different conditions

From the picture, it is found that the strength of the vortex is the largest, and its range is also wide. Furthermore, it is dominated by the reverse vortex, and this may lead to the unstable operation of the pump which can cause vibration and noise. Under the over load condition, the flow separation appears frequently in the backside of the impeller, and produces the vortex which corresponds with the rotation direction. Meanwhile, when the blade outlet angle is too big, the distribution of the regularization helicity becomes disordered, and it results in the increase of the wake region which swept by the impeller, and this may easily form the diffusion losses. Besides, when the angle increases to  $47^\circ$ , there are both positive vortex and reverse vortex in the flow field, and their intensity is quite large.

*3.2.2. The reflux characteristics under the part load condition.* The axial velocity vector under 0.6Q is shown in the figure 4. From the picture, it is found the reflux occurs in the four impellers and mainly concentrates near the wall. The reflux is not obvious at the angle of  $27^\circ$ , and its range is relatively

small. Then, with the increase of the blade outlet angle, the reflux becomes intense. This is due to the fact that although all the outlet area of the impellers are the same, the increase of blade outlet angle will have a certain effect on the work of the fluid, and even lead to the blockage, which can directly induce the reflux. Therefore, seeing the figure 4(d), the reflux vortex is the biggest at the angle of  $47^\circ$ , and it mainly distributes along the wall.

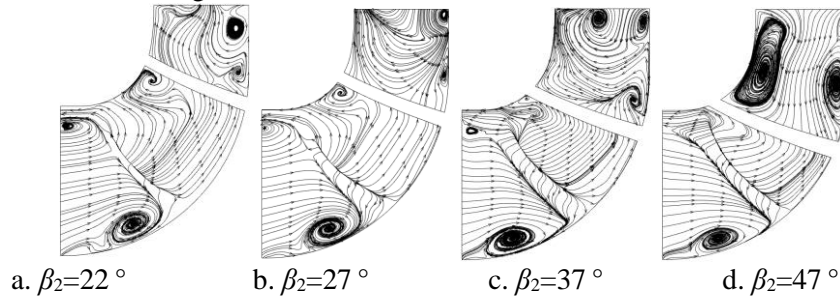


**Figure 4.** Axial velocity vector in impeller with different outlet angle under  $0.6Q$

### 3.3. The effect of the blade outlet angle on the pressure fluctuation

**3.3.1. Layout of monitoring point.** In this paper, the pressure fluctuation of two key positions in the middle section of the volute was monitored. Its coordinate is as shown in the Figure 6. P1, R=188mm,  $\theta=81^\circ$ ; P2, R=246mm,  $\theta=0^\circ$

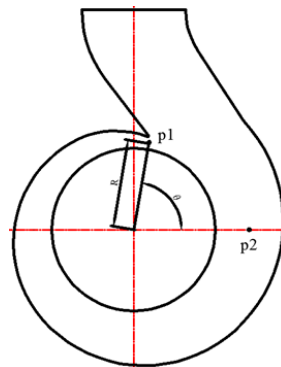


**Figure 5.** Monitoring points on middle section of volute

**3.3.2. Time domain analysis.** The static pressure of the two positions were acquired through the unsteady calculation, and the pressure coefficient was used for the quantitative comparison of the pressure fluctuation. It was defined as:

$$C_p = \frac{p - \bar{p}}{\frac{1}{2} \rho u_2^2} \quad (4)$$

Where,  $p$  presents the real-time static pressure of the monitors,  $\bar{p}$  is the average static pressure of the monitors,  $\rho$  is media density, and  $u_2$  is circumferential velocity.

Figure 6 shows the time domain analysis of the pressure fluctuation of the two monitors in a cycle under the partial conditions for the different angles. It is found that the jet wake at the baffle tongue is pretty obvious under the over load condition, so the amplitude of the pressure fluctuation is quite big. Except for the blade outlet angle of  $47^\circ$ , the waveform of other three schemes is basically the same, and this could indicate the pressure fluctuation was mainly influenced by the interaction of the blades and baffle tongue. However, if the blade outlet angle is too big, it could have a significant effect on the waveform, and even change the dominate frequency.

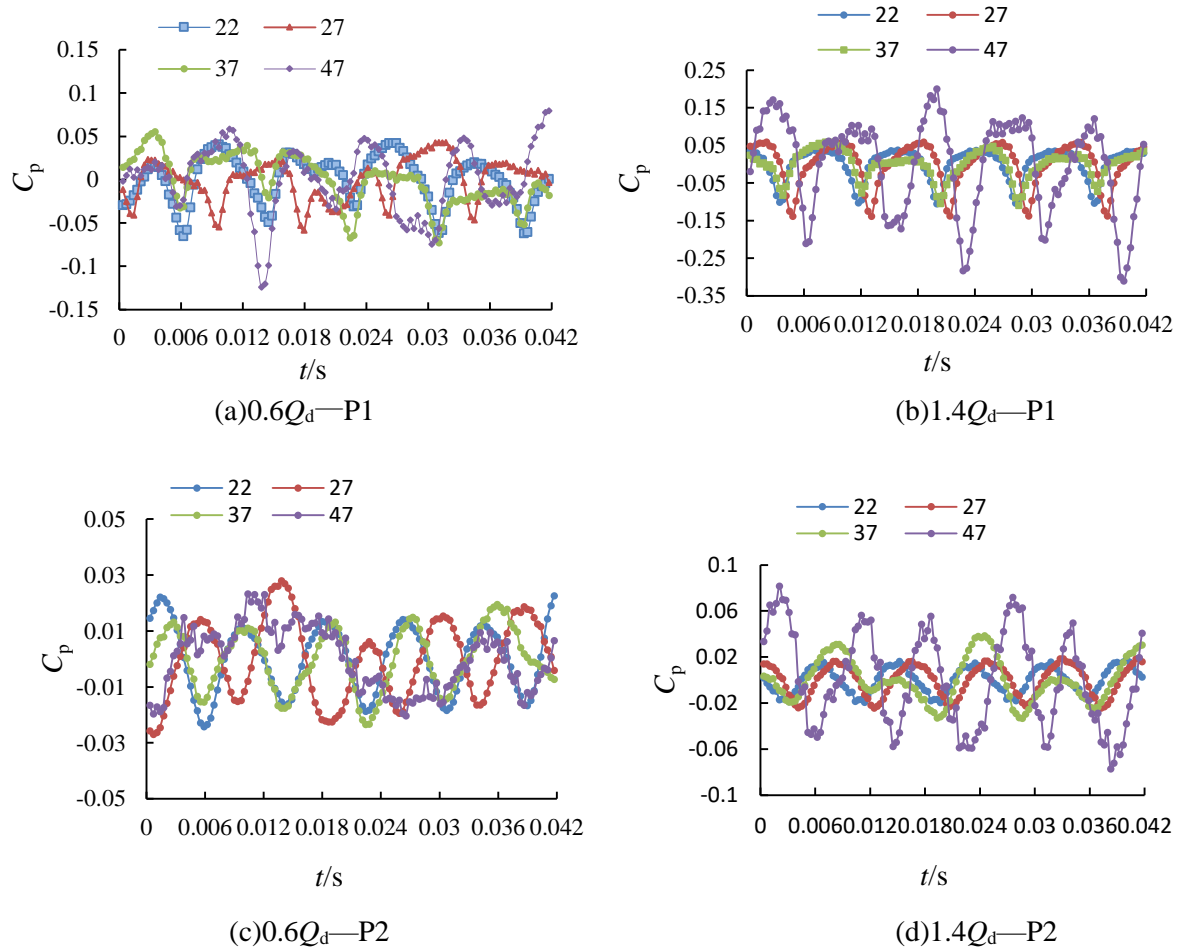


**Figure 6.** Comparisons of pressure fluctuation in time domain of monitor points in volute under partial conditions

#### 4. Analysis on structural dynamic characteristics

##### 4.1. Structure domain analysis

In the actual operation of the pump, the deformation of the solid domain will result in changes of the distribution of flow field inside the pump, at the same time, the unsteady flow of fluid field can lead to the deformation of the solid domain. The bi-directional coupling fluid-structure interaction (FSI) simulation was applied for the 4 schemes under the designed condition. The boundary line of the shroud with the blade face and blade back were respectively defined as “PS” and “PH”. Also, the boundary line of the hub with the blade face and blade back were respectively defined as “SS” and “SH”.

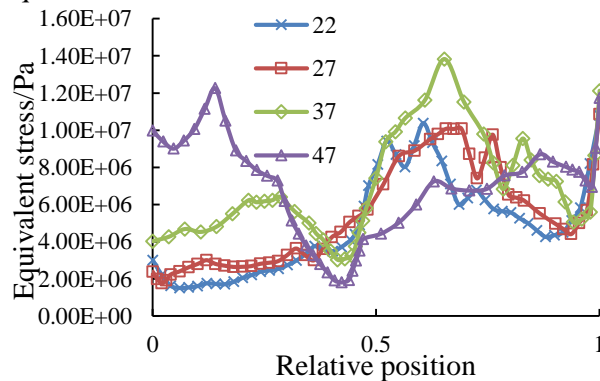
**4.1.1. The distribution of equivalent stress at the boundary line.** In this paper, the equivalent stress which was defined by the fourth strength theory was introduced to analyse the distribution of the dynamic stress, and its definition formula is as follow:

$$\sigma_{\text{eq}} = \sqrt{\frac{1}{2} \left[ (\sigma_x - \sigma_y)^2 + (\sigma_y - \sigma_z)^2 + (\sigma_z - \sigma_x)^2 \right]} \quad (5)$$

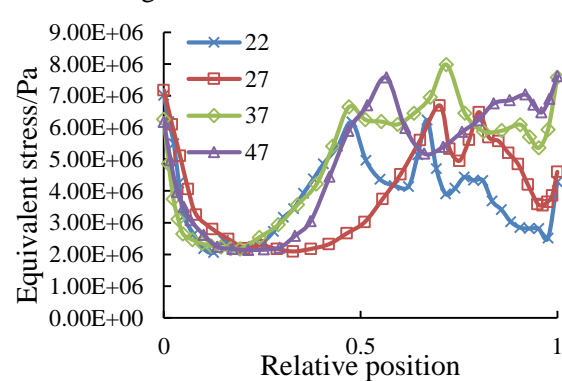
Where, the  $\sigma_x$ ,  $\sigma_y$  and  $\sigma_z$  represent the first main stress, the second main stress and the third main stress respectively.

The figure 7 shows the distribution of the equivalent stress at the boundary line “PS” in 4 impellers with different blade outlet angle under the designed condition. It can be seen that the equivalent stress of the 4 schemes all increase along the flow direction; meanwhile, the uniformity of the equivalent stress decrease with the increase of the blade outlet angle; the equivalent stress is particular big when the blade outlet angle is 47° near the inlet, and there is a minimum appears in the position of 0.4 times at the outlet; On the whole, for other 3 schemes, there is an obvious fluctuation phenomenon in the position of 0.6 times to 0.8 times at the outlet; the equivalent stress concentration is relatively common near the outlet.

The figure 8 shows the distribution of the equivalent stress at the boundary line “PH” in 4 impellers with different blade outlet angle under the designed condition. It can be seen that the distribution of the equivalent stress near the inlet of the 4 schemes is approximate, and there is a minimum in the position of 0.2 times at the outlet; the equivalent stress are relatively lower near the outlet when the blade outlet angle are 22° and 27°; From the position of 0.8 times at the outlet, the equivalent stress increases with the increase of the blade outlet angle.



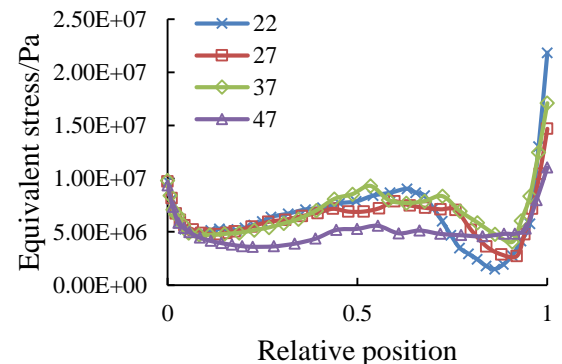
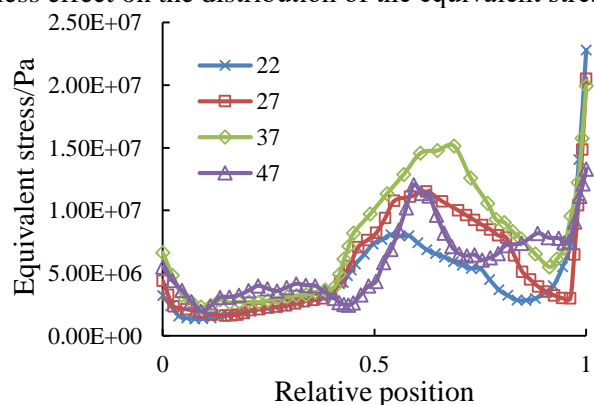
**Figure 7.** Equivalent stress distribution of the boundary line PS



**Figure 8.** Equivalent stress distribution of the boundary line PH

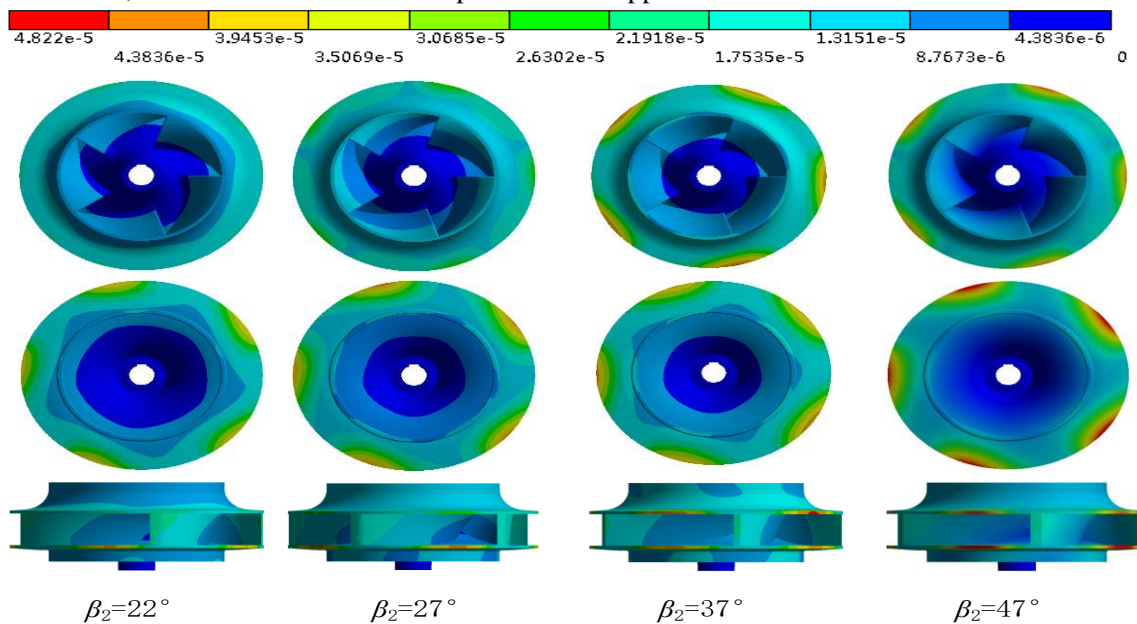
The figure 9 shows the distribution of the equivalent stress at the boundary line “SS” in 4 impellers with different blade outlet angle under the designed condition. It can be seen that comparing with picture 5.5, the equivalent stress of the 4 schemes are relatively stable from the inlet to the position of 0.4 times at the outlet, and the same is the equivalent stress concentration phenomenon near the outlet. On the whole, the blade outlet angle has less effect on the distribution of the equivalent stress at the boundary line “SS” than “PS”.

The figure 10 shows the distribution of the equivalent stress at the boundary line “SH” in 4 impellers with different blade outlet angle under the designed condition. It can be seen that the distribution of the equivalent stress is similar to the boundary line “SS”, and the blade outlet angle has less effect on the distribution of the equivalent stress at the boundary line “SH”.

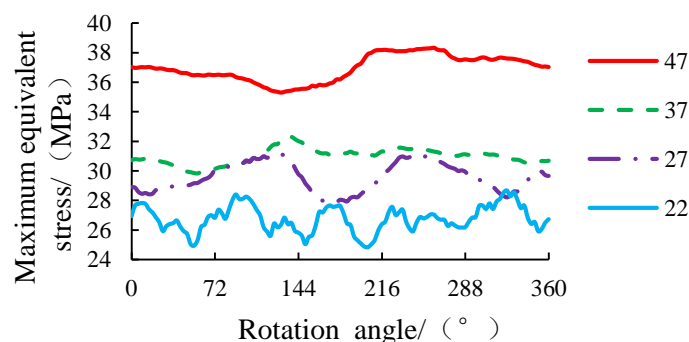


**Figure 9.** Equivalent stress distribution of the boundary line SS**Figure 10.** Equivalent stress distribution of the boundary line SH

**4.1.2. Deformation distribution analysis of impeller.** The figure 11 shows the deformation distribution of the impellers with different blade outlet angle under the designed condition. It can be seen that the deformation is small near the wheel hub, because the wheel hub is thick, and it is not easily affected by the stress. Meanwhile, the deformation of the shroud is generally less than the hub, especially at the blade outlet angle of  $22^\circ$  and  $27^\circ$ . In addition, with the increase of the blade outlet angle, the deformation area increases gradually, and it mainly concentrates on the outlet. This phenomenon may be because of the influence of the jet wake at the outlet, and the obvious pressure difference acts on the solid domain, so the stress concentration phenomenon appears.

**Figure 11.** Total deformation of impeller under design condition (unit: m)

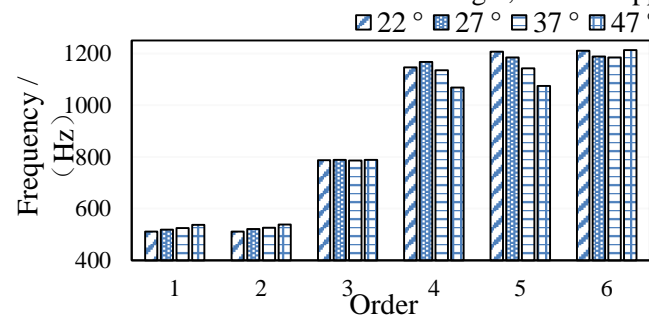
**4.1.3. Time domain analysis of equivalent stress.** The figure 12 shows that the time domain analysis of the maximum equivalent stress for the 4 schemes under the designed condition. With the increase of the blade outlet angle, the maximum equivalent stress rises, but its strength decreased. In addition, the maximum equivalent stress is basically stable at 37 MPa with the blade outlet angle of  $47^\circ$ , and when the angle is  $22^\circ$ , the fluctuation of the maximum equivalent stress is most intense. The above analysis, we can find that the blade outlet angle could not be too big or small. When it is too big, the maximum equivalent stress may reach the ultimate stress of the structure. If it is too small, it may lead to obvious alternating dynamic load, and this could cause the fatigue failure.



**Figure 12.** Time domain analysis of maximum equivalent stress of impeller under designed condition

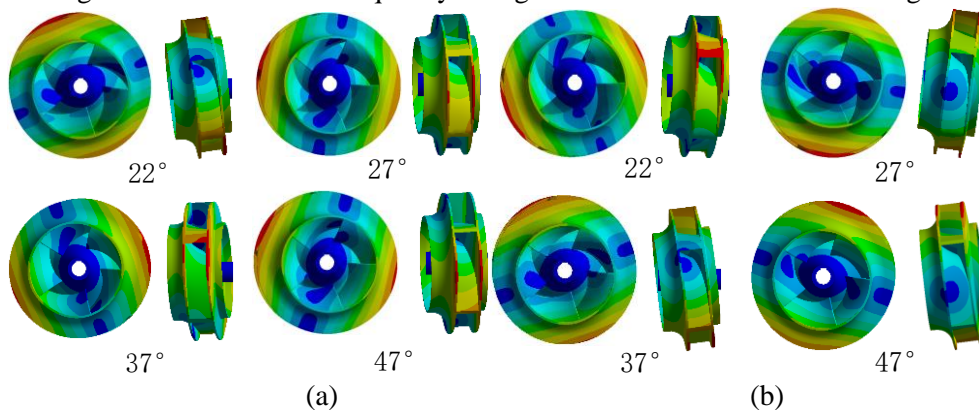
#### 4.2. Wet mode characteristic

The natural frequency before six order under the wet mode for the different blade outlet angle is shown in figure 13. It can be seen that the first order natural frequency for the 4 impellers are all higher than 500Hz, which is much higher than the blade passing frequency of the model pump. Meanwhile, it avoids the frequency of second harmonic and third harmonic, and the resonance phenomenon caused by the periodical flow incentive would not appear. Additionally, in the first and second order, the natural frequency increases with the increase of blade outlet angle, but it is opposite for the fifth order.



**Figure 13.** Influence of blade outlet angle on the natural frequency of wet mode

Figure 14 shows the vibration mode in the first, second, fourth and fifth wet mode for the four impellers. The figure 14(a) and 14(b) show the radial swinging vibration mode of the first two order, and the largest deformation both appear in a symmetric position of the impeller. Figure 14(c) and 14(d) show the axial swinging vibration mode of the fourth and fifth order. Seeing from the figure 14(c), the swinging amplitude for the blade outlet angle is relatively small, and equally distributed. But for 37° and 47°, their axial swinging are obvious, and the direction are different. The swinging amplitude are further intensified for the four impellers, and the blade outlet angle is smaller, the swinging amplitude is larger. This is similar to frequency changes in the fifth order showed in figure 13.



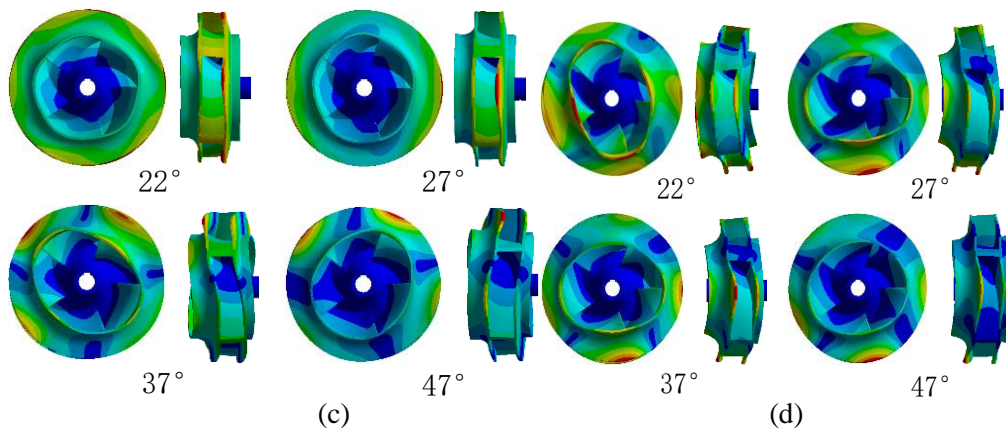


**Figure 14.** Vibration of structure for impeller with different blade outlet angle

## 5. Conclusion

In this study, a single-stage and single-suction chemical centrifugal pump with the specific speed of 180 was analysed by simulation and test, and the three other impellers with different blade outlet angle were designed based on the model pump. Then, these schemes were analysed from several aspects to find the effect of the blade outlet angle on the chemical centrifugal pump, and the conclusions were as follows:

Under the designed condition, the head rose with increase of the blade outlet angle. But if the angle was too big, the head would drop sharply under the over load condition.

Under the part load condition, the reflux became more intense with the increase of the blade outlet angle, and it mainly appeared at the shroud or hub. This is the same as predicted by the regularization helicity.

The equivalent stress on the boundary line of the blade face and the shroud in the position of 0.6 times to 0.8 times at the outlet were greatly affected by the blade outlet angle. For the hub, from the position of 0.8 times at the outlet, the equivalent stress rose with the increase of the blade outlet angle.

Through the two-way coupled fluid-structure interaction (FSI) simulation, the deformation is small near the wheel hub, and the deformation of the shroud is generally less than the hub. The appropriate reduction of the blade outlet angle would reduce the deformation, and improve its distribution.

## References

- [1] Huang Liequn, Wu Peng, Xue Cunqiu, et al. Review of progress on the design technology of centrifugal type chemical process pump[J]. *Mechanical Electrical Engineering Magazine*, 2009(06):1-4.
- [2] Huang Xi, Yuan Shouqi, Zhang Jinfeng, et al. Effects of blade wrap angle on performance of high-specific-speed centrifugal pump[J]. *Journal of drainage and irrigation machinery engineering*, 2016, 34(9):742-747.
- [3] Zhang Jinfeng, Yuan Shouqi, Fu Yuedeng, et al. Numerical Forecast of the Influence of Splitter Blades on the Flow Field and Characteristics of a Centrifugal Pump[J], *Journal of Mechanical Engineering*, 2009,(07):131-137. (in Chinese)
- [4] Pei J, Yuan S, Benra F K, et al. Numerical Prediction of Unsteady Pressure Field Within the Whole Flow Passage of a Radial Single-Blade Pump[J]. *Journal of Fluids Engineering*, 2012,134(10):101103.
- [5] Bacharoudis E C, Filios A E, Mentzos M D, et al. Parametric Study of a Centrifugal Pump Impeller by Varying the Outlet Blade Angle[J]. *Open Mechanical Engineering Journal*, 2008,2(1):75-83.
- [6] Zha Sen. The Principle and Hydraulic Design of Vane Pump [M]. *China Machine Press*, 1988.
- [7] ShenYang Pump Research Institution. Vane pump Designing Manual [M]. *China Machine*

*Press*, 1983.

- [8] Guan Xingfan. Modern Pump Theory and Design[M].*China Astronautics Press*, 2011.
- [9] Veselov V I. Effect of the Outlet Angle  $\beta_2$  on the Characteristics of Low Specific-speed Centrifugal Pumps[J]. *Power Technology and Engineering*, 1982,16(5):267-273.
- [10] Li W, Shi W D, Jiang T, et al. Analysis on Effects of the Blade Wrap Angle and Outlet Angle on the Performance of the Low-Specific Speed Centrifugal Pump[J]. *Advanced Materials Research*, 2011,354-355:615-620.
- [11] González J, Santolaria C. Unsteady Flow Structure and Global Variables in a Centrifugal Pump[J]. *Journal of Fluids Engineering*, 2006,128(5):937-946.
- [12] Worster R C. The flow in volutes and its effect on centrifugal pump performance[J]. *ARCHIVE Proceedings of the Institution of Mechanical Engineers* 1847-1982 (vols 1-196), 1963,177(1963):843-875.